ABUAD Journal of Engineering Research and Development (AJERD)
ISSN (online): 2645-2685; ISSN (print): 2756-6811

Volume 7, Issue 1, 231-240

Performance Analysis of Inverter Fed Single Phase Induction Motor Drive

Gerald Chidozie DIYOKE[1], Candidus Ugwuoke EYA[2], Patrick Ifeanyichukwu OBI[1], Ifeanyichukwu Kalu ONWUKA[1]

[1]*Department of Electrical & Electronic Engineering, Michael Okpara University of Agriculture, Umudike, Nigeria*
geraldiyoke@mouau.edu.ng/patndyobi@gmail.com/onwuka.ifeanyi@mouau.edu.ng

[2]*Department of Electrical Engineering, University of Nigeria, Nsukka, Nigeria*
Candidus.eya@unn.edu.ng

Corresponding Author: geraldiyoke@mouau.edu.ng, +2348032886906
Date Submitted: 25/03/2024
Date Accepted: 17/05/2024
Date Published: 05/06/2024

Abstract: *This paper presents performance analysis of effects of modulation index on cascaded multilevel inverter fed single phase induction motor drive using closest level control technique. The modulation index is varied to analyze its performance. The effects on inverter output voltage, current, induction motor speed, electromagnetic torque and total harmonic distortion (THD) are considered. Both the load torque and modulation index are varied to determine the motor performance. The Closest (Nearest) control method is applied for generating firing pulses for the cascaded multilevel inverter power switches. By the application of this method, the switching losses are greatly mitigated when compared with high switching frequency of Pulse Width Modulation (PWM) schemes. MATLAB/SIMULINK software is used to obtain the system simulation results. The performance evaluation of this work was targeted on the modulation index range from 0.7 to 1.2 and for selected load torque values of 0 Nm, 2 Nm and 4 Nm. It is observed that modulation index affects the motor performance. When modulation index is 1.0 under different load torques, 6.2 % - 6.7 % range of voltage THD was obtained. When the modulation index becomes 1.2, motor speed and electromagnetic torque resulted to 1327 RPM and 20 Nm respectively with stability time of 0.7 sec under load torque of 4 Nm.*

Keywords: *Closest Level Control, Induction, Hybrid Topology, Multilevel Inverter, Single-phase.*

1. INTRODUCTION

In industrial applications, higher voltage and current drives are indeed needed for optimal performance of the many electrical systems. There is a geometric increase in the demand of electrical energy [1). Based on that condition, the amount of resources and different sources of energy required to address these issues of power demand both industrial and domestic usage also increase. Higher power ratings, improved efficiency, low power electronics component counts and low harmonic distortion with cost reduction are the most core concept of industrial and commercial drivers [2]-[4]. Micro sources of electrical energies such as fuel cells, photovoltaic (PV) systems, and batteries are all alternative sources of energy generations which are all renewables' sources ([5] and [6]. The systems can be interconnected or synchronized with the help of power electronics converters such as ac-dc, dc-dc, dc-ac or ac-ac converters.

Inverters are part of power system conversions that can convert regulated or unregulated dc to a regulated ac system through the means of modulations. They are grouped in terms of single, three and multi-phases. Power DC-AC converter can also be grouped based on configurations namely: conventional and multi-levels. Voltage and current sources inverters are also available. In terms of modulation schemes for inverters, they are divided based on single pulse width modulations, multiple pulse width modulation, sinusoidal pulse width modulation and space vector pulse width modulation. Due to numerous merits of multilevel inverter, it is adopted in the work [7]. The advantages are basically focused on the output quality and nominal power increase in the inverter improvements [8]. Multilevel inverter configuration has proven very attractive to the industry due to its novel properties. In recent time, researchers and scholars all over the world are spending great efforts toward improving the performance of multilevel inverter families by simple control with reduced number of components and optimized algorithms in order to decrease THD and torque ripple of the motor. The first three generally accepted members of multilevel inverter configurations are diode clamped, flying capacitor, and cascaded H-bridge. As reported, Diode clamped Multilevel Inverter is a very general and widely used topology for real power flow control [8]. In applications for high-power medium-voltage drive, due to the ability of the power circuit structure to lower the voltage ratings of the power switches, multilevel converters are also considered [10], [11]). In order to reduce the power component counts and voltage harmonics, a transistor clamped H-bridge (TCHB) inverter is adopted on the work. To enhance the output voltage and allow more energy-mix technology, a cascaded topology of this circuit is considered and adopted for this research work.

In recent time, AC induction motors are preferred in almost all industrial drives [12]. The AC motors have good merits over others such as: low cost, rugged, reliable, and relatively inexpensive with high efficiency. Due to the aforementioned properties, induction motors are mostly preferable in many areas of industrial control applications [13]. Nowadays, due to advancement in power electronics and drives, mechanical gear systems are now replaced by this technology. This improved technology is applied for variable motor speed drives control and under dynamic and steady state conditions, the speed and torque characteristics response performance of the motor can be improved [14]. The variable frequency operation is required for adjustable AC motor drive applications. So that AC drive system is fed from the power electronic converters [15]. For conversion of fixed voltage and frequency to variable voltage and frequency, power electronic converters are suitable and then AC motor speed control.

In orders to achieve an adjustable speed control of induction motors and better commutation of the power inverter, the nearest level modulation is utilized. Different types of this modulation technique are investigated adding carriers in each level with level shifted PWM as reported [16], phase shifted PWM [17], or using different carrier frequencies [18]. Comparison algorithm to calculate the switching pattern in the high voltage cells, and a carrier-based modulation to the smaller one has been applied in hybrid modulation technique [19]. Asymmetry factors are the functions of the performance of this modulation scheme [20] and can present over-modulation [21]. A novel modulation scheme is proposed in [22] to be applied when the DC supply voltages does not have integer ratio. The report on [23] targeted on the mathematical analysis of the power distribution in each cell; and the regeneration of small voltage cells, establishing the rates where it is produced when a nearest level modulation is used.

The rest of the paper are structured as follows, section 2 is about the approach to the paper which includes circuit topology, induction motor and control scheme analysis, section 3 presents MATLAB/SIMULINK simulation results of the system and conclusion is presented in section 4.

2. METHODOLOGY

This research work involves a hybrid cascaded multilevel inverter, single phase induction motor, control scheme.

2.1 Circuit Topology

In this research work, regulated DC input voltage is used as DC voltage source. The cascaded hybrid multilevel inverter power circuit is as depicted in Figure 1. The single-phase induction motor is connected as the load. Thirteen different output phase voltage levels are obtained as the supply voltage to the motors as shown in Table 1. The power circuit is made up of two similar cells with different input voltage values. Figure 2 depicts the detailed waveforms of the voltage for each cell as well as for the inverter output voltage otherwise called motor supply voltage. The sum of individual cell output voltages gives the output voltage delivered to the motor.

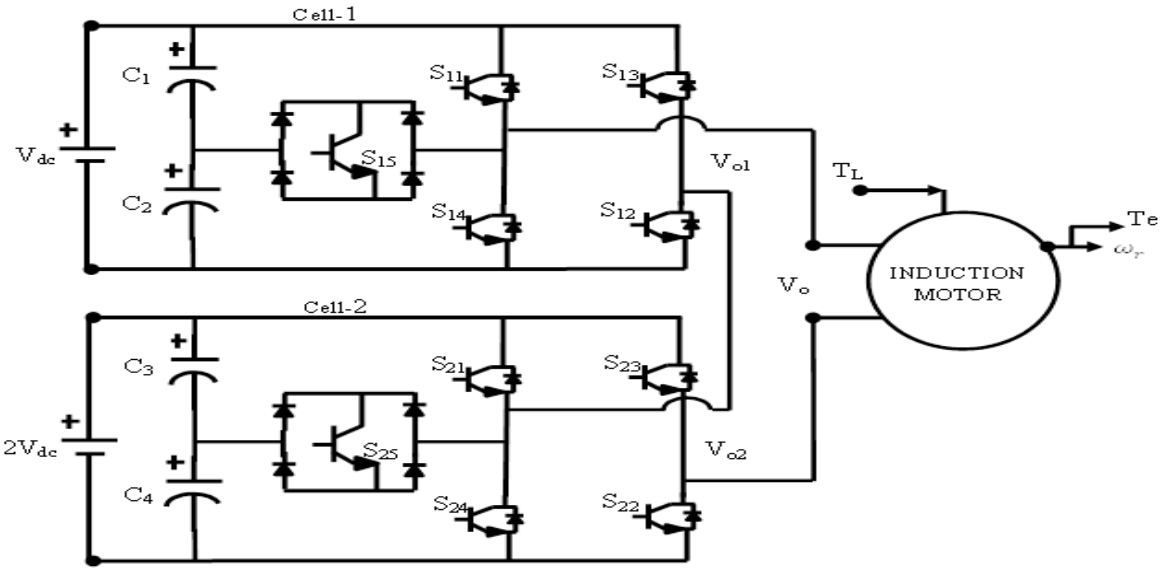

Figure 1: The proposed asymmetrical TCHB inverter topology [24] and [25] with induction motor load

The inverter output voltages per cell for different switching state are given as:

$$V_{o1} = V_{dc}(S_{12} - S_{13})\left\{\frac{1}{2}S_{15} + (|S_{11} - S_{13}| \cdot |S_{12} - S_{14}|)\right\} \quad (1)$$

$$V_{o2} = 2V_{dc}(S_{22} - S_{23})\left\{\frac{1}{2}S_{25} + (|S_{21} - S_{23}| \cdot |S_{22} - S_{24}|)\right\} \quad (2)$$

When only one cell is considered, the inverter operation of the power circuit is divided into five different switching modes as reported by [25].

Table 1: Switching pattern of the TCHB, ON: 1, OFF: 0.

State	S_{11}	S_{12}	S_{13}	S_{14}	S_{15}	S_{21}	S_{22}	S_{23}	S_{24}	S_{25}	V_o (V_{dc})
1	1	0	1	0	0	1	0	1	0	0	0
2	0	0	0	0	0	0	1	0	0	1	$\frac{1}{2}$
3	0	0	0	0	0	1	1	0	0	0	1
4	0	0	0	0	0	1	1	0	0	1	$1\frac{1}{2}$
5	0	1	0	0	1	1	1	0	0	0	2
6	1	1	0	0	0	0	1	0	0	1	$2\frac{1}{2}$
7	1	1	0	0	0	1	1	0	0	0	3
8	0	1	0	1	0	0	1	1	1	0	0
9	0	0	0	0	0	0	0	1	0	1	$-\frac{1}{2}$
10	0	0	0	0	0	0	0	1	1	0	-1
11	0	0	0	0	0	0	0	1	1	1	$-1\frac{1}{2}$
12	0	0	1	0	1	0	0	1	1	0	-2
13	0	0	1	1	0	0	0	1	0	1	$-2\frac{1}{2}$
14	0	0	1	1	0	0	0	1	1	0	-3

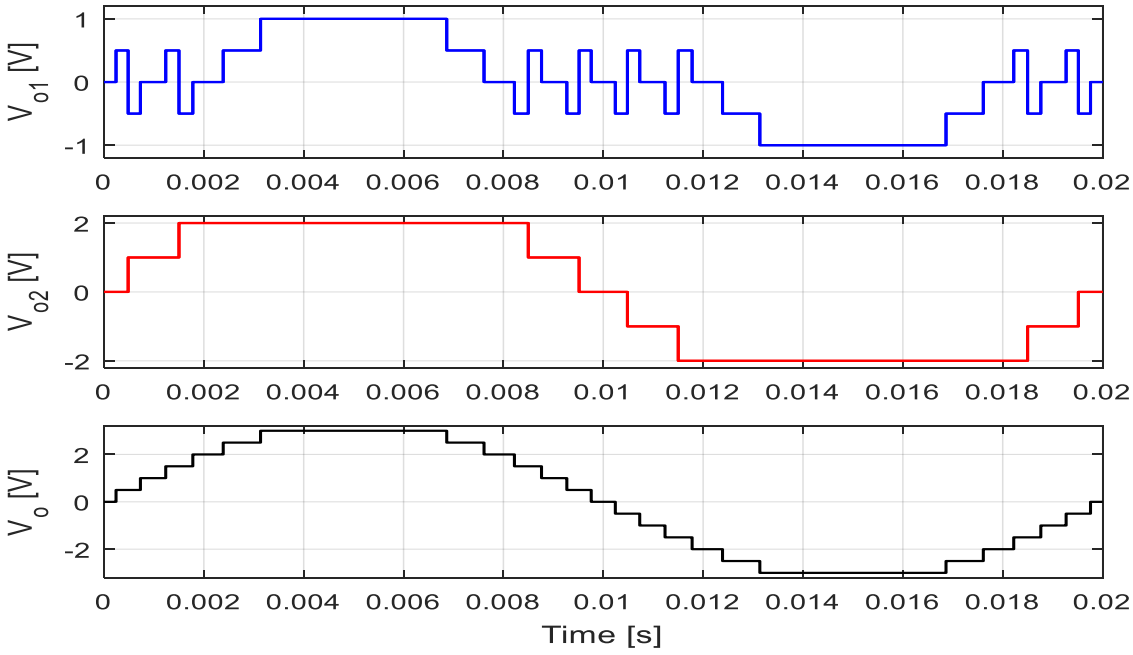

Figure 2: Waveforms for low-voltage cell, high-voltage cell, and resultant output voltages, respectively

Many commutations per cycle are observed in low-voltage cell unlike the high-voltage cell as depicted in Figure 2. The cell 2 delivers most of the power due fundamental frequency commutation. As a result of this act, the switching losses are reduced significantly in the system. Detailed switching signals for each power switch are illustrated in Figure 3. Cell 1 shows low switching frequency while cell 2 depicts high switching frequency.

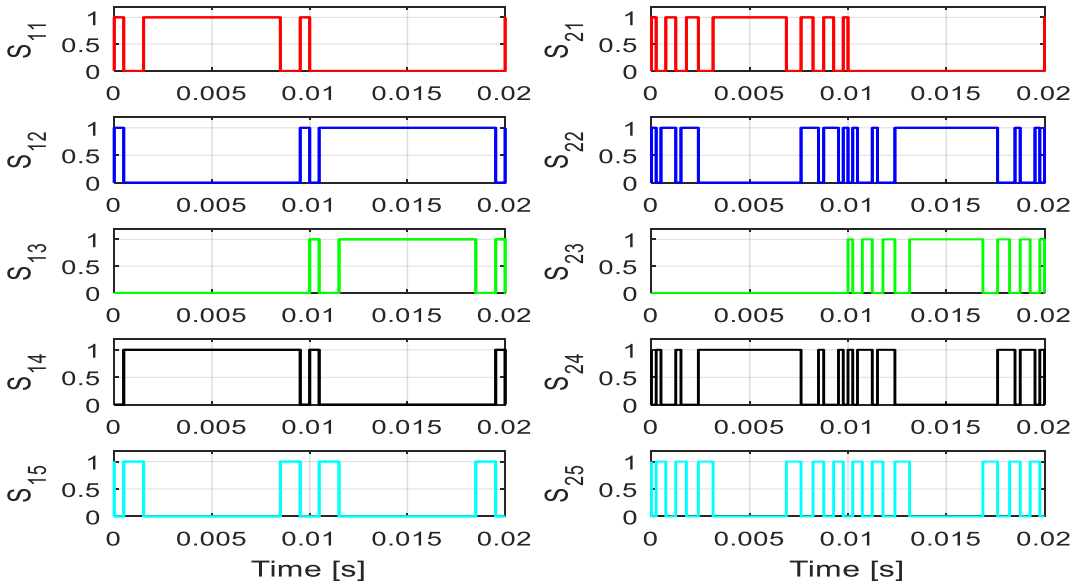

Figure 3: Individual switching signals for TCHB inverter circuit.

2.2 Proposed Control Scheme

The proposed control method is adopted from [23] and [24]. The modulation index, M is defined as a ratio of reference amplitude to the total DC link voltage, V_m of the cells. For the high-voltage cell, the reference amplitude is given by Equation (3);

$$V_{r2} = MV_m sin\omega t \tag{3}$$

The voltage reference V_{r2} is compared with the two constants $h_{L,2}$ and $h_{H,2}$. Then the firing signals are generated to the switches of the high-voltage cell using logic gates. For the low-voltage cell, the reference signal is generated by Equation (4);

$$V_{r1} = V_{r2} - (2h_{L,2} \times L_2) \tag{4}$$

Where L_2 is the switching pattern resulting from the high-voltage cell after comparison and is given as Equation (5);

$$L_2 = [(V_{r2} > h_{L,2}) + (V_{r2} > h_{H,2})] - [(V_{r2} < h_{L,2}) + (V_{r2} < h_{H,2})] \tag{5}$$

In the same way, L_1 switching pattern for low-voltage cell is generated as Equation (6);

$$L_1 = [(V_{r1} > h_{L,1}) + (V_{r1} > h_{H,1})] - [(V_{r1} < h_{L,1}) + (V_{r1} < h_{H,1})] \tag{6}$$

The total inverter output voltage, V_o is generated by the combination of Equations. (3) and (4), which is mathematical expressed as

$$V_o = (L_1 + L_2) \times V_{dc} \tag{7}$$

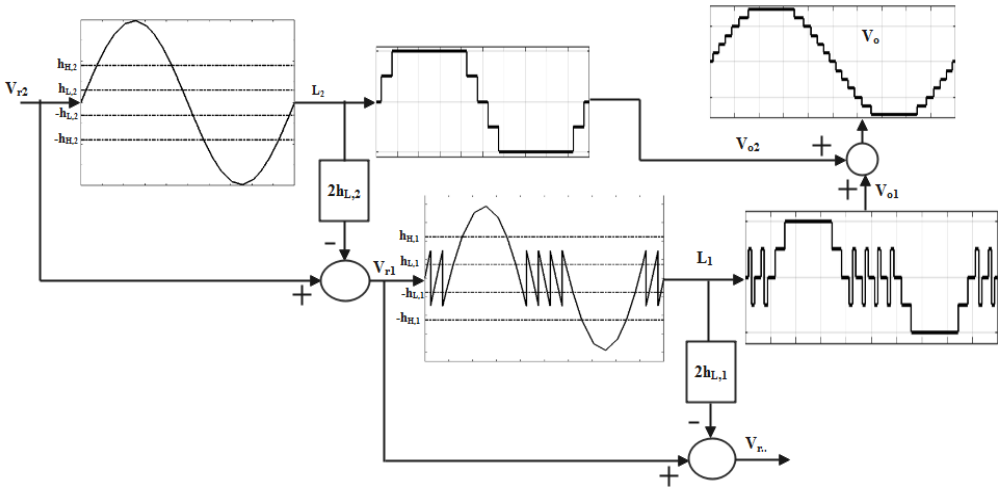

Figure 4: Implementation of the nearest level control method.

2.3 Analysis of Motor input Voltage

The motor input voltage waveform $V_o(\omega t)$ is obtained from the general Fourier expression in Equation (8); thus, the voltage can be expressed using Fourier series as:

$$V_o(\omega t) = \frac{a_o}{2} + \sum_{n=1,2,3}^{\infty}(a_n cosn\omega t + b_n sinn\omega t) \quad (8)$$

The Fourier coefficient b_n for odd function can be expressed by Equation (9) since all even functions are equal to zero [24].

$$b_n = \frac{2V_{dc}}{n\pi}\sum_{i=1,2,3}^{S} cosn\theta_i \quad (9)$$

Substituting Equation (9) into Equation (8) yields

$$V_o(\omega t) = \sum_{n=1,2,3}^{\infty}\left(\frac{2V_{dc}}{n\pi}\sum_{i=1,2,3}^{S} cosn\theta_i\right) sinn\omega t \quad (10)$$

where the number of switching angles in a quarter-wave is denoted as S and the switching angles which lies between zero and 90^o is represented by θ_i. The switching angles can be computed using the formulae in [24] and [26]. Equation (10) depicts the stator supply voltage from the cascaded multilevel inverter output voltage. The steady state analysis of electrical motors is well detailed in [27]. Steady-state torque is the torque exerted on a rotating component to counteract all resistive forces and maintain a constant speed under steady operating conditions. In an ideal scenario with no external disturbances, the steady-state torque is equal to the torque required to overcome friction and other resistive forces acting on the system. In this work, the effect of load torque variation on the motor speed is well detailed.

3. RESULTS AND DISCUSSIONS

Simulation procedures were carried out in MATLAB/SIMULINK software to validate the proposed technique. The circuit topology of the simulated improved multilevel inverter fed induction motor drive as depicted in Figure 1 with control technique as shown in Figure 4. The simulation parameters are shown in Table 2. To obtain comprehensive performance evaluations, the system behaviour was tested under constant load torques with variations in the modulation index.

3.1 Simulation Results on no Load Torque with a Variable Modulation Index

As shown in Figure 5, the output voltage levels from the improved multilevel inverter fed IM with NLC technique were obtained at variable modulation indices of 0.7, 0.8, 0.9, 1.0 and 1.2 with zero load torque. The result obtained shows that at M = 1.2 and M = 1.0 delivered the same voltage amplitude of 180 V, while at M = 0.9 and M = 0.8 showed the same voltage magnitude of 150 V. At M = 0.7, a value of 120 V output voltage was obtained. Figure 6(a) shows the machine transient behaviour of the rotor current at zero load torque with variable modulation indices, the rotor current shows a peak value of 24 A at M = 1.2 and 18 A at M = 0.7. The rotor current stability was considered between time interval of 2.4 s to 2.45 s, at M = 1.2; therefore, a 2.48 A rotor current was obtained as depicted in Figure 6(b). Figure 7 shows the effects of different modulation indices at no load torque on the motor speed. At M = 1.2 the motor achieved stability before 0.5 s while at M = 0.7 the motor speed attained stability at 1 s with rate speed value of 1500 RPM. The waveforms of electromagnetic torque against time were obtained as depicted in Figure 8. Figure 8(a) shows the plot at M = 0.7 with maximum torque value of 8 Nm. Figure 8(b) shows the plot at M = 0.8 with maximum torque value of 10 Nm. At M = 0.9, a maximum torque value of 12 was obtained as depicted in Figure 8(c). At M = 1, a maximum torque value of 15 was obtained as depicted in Figure 8(d). Figure 8(e) shows the plot at M = 1.2 with maximum torque value of 20 Nm. It is observed the increased in modulation index increases motor speed and electromagnetic torque.

3.2 Simulation results on load torque of 2 Nm with a variable modulation index

As shown in Figure 9, the output voltage levels from the improved multilevel inverter fed IM with NLC technique were obtained at variable modulation indices of 0.7, 0.8, 0.9, 1.0 and 1.2 with 2 Nm load torque. The result obtained shows that at M = 1.2 and M = 1.0 delivered the same voltage amplitude of 180 V, while at M = 0.9 and M = 0.8 showed the same voltage magnitude of 150 V. At M = 0.7, a value of 120 V output voltage was obtained. Figure 10(a) shows the machine transient behaviour of the rotor current at 2 Nm load torque with variable modulation indices, the rotor current shows a peak value of 24 A at M = 1.2 and 18 A at M = 0.7. The rotor current stability was considered between time interval of 2.4 s to 2.45 s, at M = 1.2; therefore, 2.48 A rotor current was obtained as depicted in Figure 10(b). Figure 11 shows the effects of different modulation indices at 2 Nm load torque on the motor speed. At M = 1.2 the motor achieved stability before 0.5 s with value of 1429 Nm. At M = 1.0 the motor attains a speed of 1409.14 rpm after 0.85 s. For M = 0.9, 1377 rpm motor speed was attained at a period of 1 s. At M = 0.8, the motor speed reached 1342 rpm at 1.5 s while at M = 0.7 the motor speed attained stability at 2 s with rate speed value of 1208 RPM. The waveforms of electromagnetic torque against time were obtained as depicted in Figure 12. Figure 12(a) shows the plot at M = 0.7 with maximum torque value of 7.6 Nm which occurred at 1. 035 s. Figure 12(b) shows the plot at M = 0.8 with maximum torque value of 10 Nm which occurred

at 0.575 s. At M = 0.9, maximum torque value of 12 Nm which occurred at 0.445 s was obtained as depicted in Figure 12(c). At M = 1, maximum torque value of 15 Nm was obtained as depicted in Figure 12(d) and it occurred at 0.355 s. Figure 12(e) shows the plot at M = 1.2 with maximum torque value of 20 Nm which occurred at the initial time. It is observed the increased in modulation index increases motor speed and electromagnetic torque.

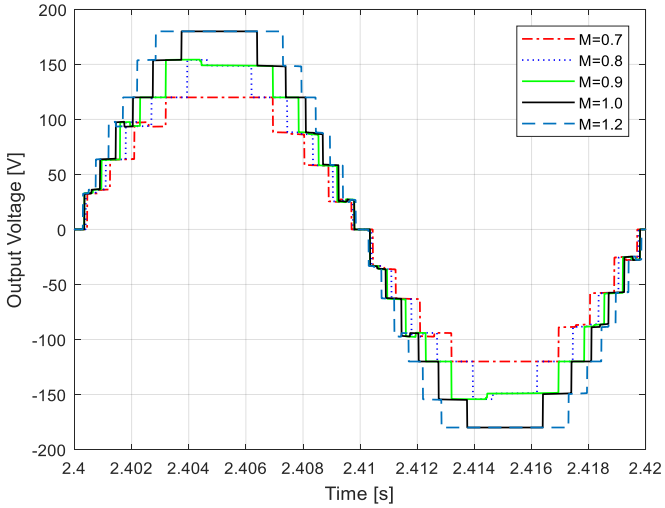

Figure 5: Inverter Output voltages at no load torque

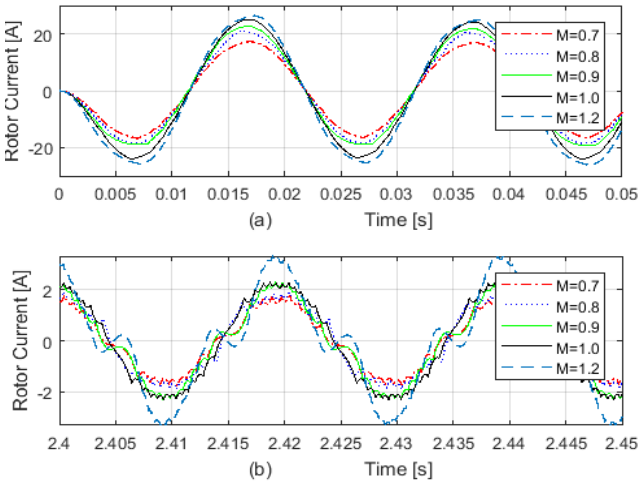

Figure 6: Inverter output current (a) transient (b) steady state.

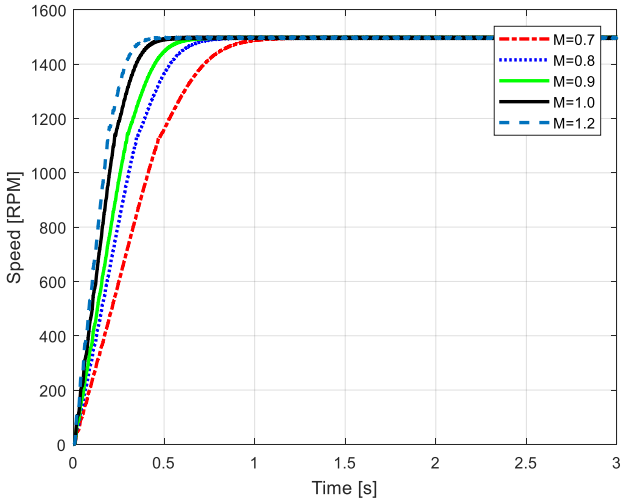

Figure 7: Motor speed at no load torque

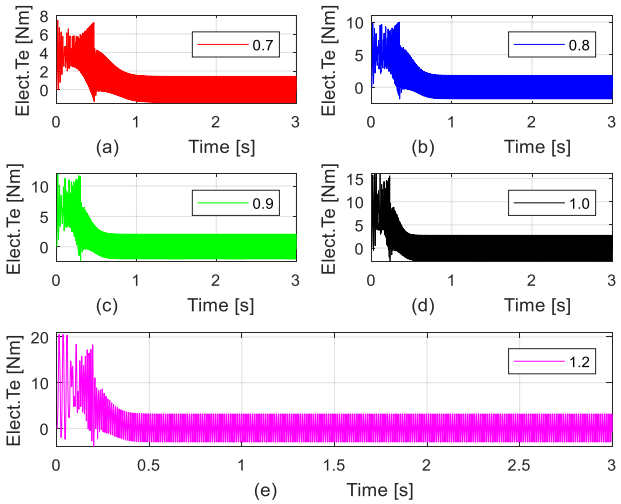

Figure 8: Electromagnetic Torque under no load condition.

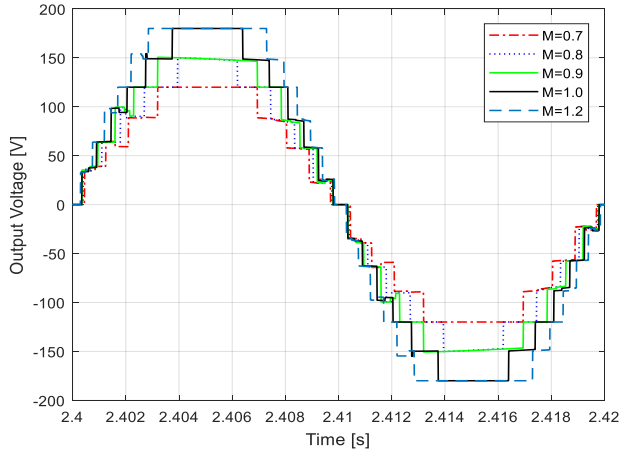

Figure. 9: Inverter Output voltages at 2 Nm load

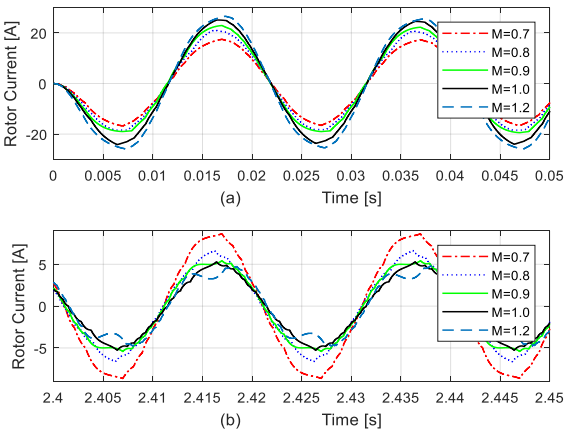

Figure. 10: Inverter output current at 2 Nm load torque (a) transient (b) steady state.

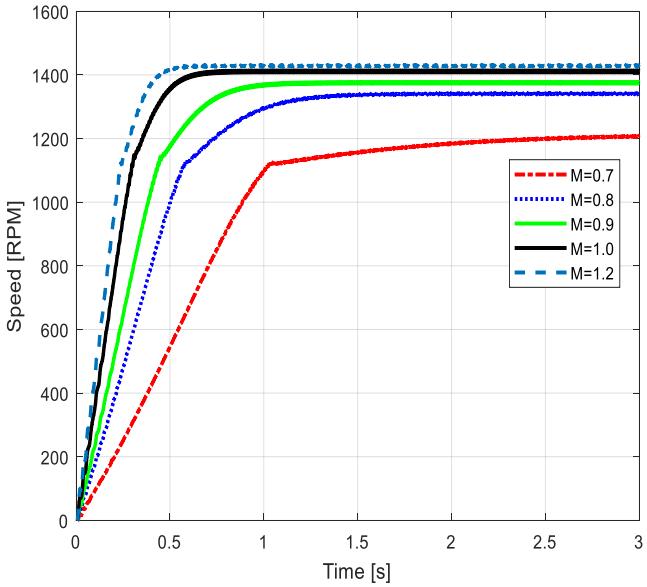

Figure 11: Motor speed at 2 Nm torque load

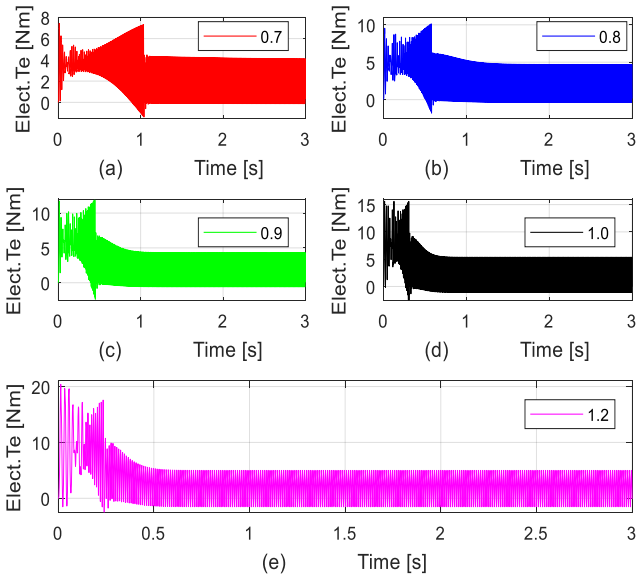

Figure 12: Electromagnetic torque under 2 Nm load condition.

3.3 Simulation results on load Torque of 4 Nm with a variable modulation index

As shown in Figure 13, the motor supply voltage shows similar characteristics as depicted in Figures 5 & 9, with load torque of 4 Nm affecting the inverter output voltages with the modulation indices of 0.7, 0.8 and 0.9. The transient waveform displayed in Figure 14(a) followed this pattern as in Figures 6(a) and 10(a). The rotor current under steady state operation is depicted in Figure 10(b) with M = 1.0 and 1.2 following the same pattern with the same amplitude and phase angle. At M = 0.7, 0.8 and 0.9 showed variable amplitudes with different phase angles. Figure 15 shows motor speed plots at different values of the modulation index. At M = 0.7 the speed took a negative value and attains a steady speed of -1930 RPM at 2.5 sec. When M becomes 0.8 the speed moves from positive to negative with maximum speed of 1125.6 RPM at 2.037 sec. At M = 0.9 the maximum speed occurred at 0.9177 sec with 1129.45 RPM, this speed changes to negative after reaching zero at 2.28 sec and stabilizes with -1630 RPM at 2.667 sec. Motor speed of 1254 RPM was attained at 0.85 sec for modulation index value of 1.0. When the modulation index becomes 1.2, motor speed resulted to 1327 RPM at 0.7 sec. The waveforms of electromagnetic torque against time were obtained as depicted in Figure 16. Figure 16(a) shows the plot at M = 0.7 with maximum torque value of 8.795 Nm which occurred at 2. 531 sec. Figure 16(b) shows the plot when M = 0.8 with maximum torque value of 10 Nm which occurred at 2.0377 s. When M = 0.9, maximum torque value of 11.85 Nm which occurred at 2.28 secs was obtained as depicted in Figure 16(c). At M = 1, maximum torque value of 15.6 Nm was obtained as depicted in Figure 16(d) and it occurred at 0.465 s. Figure 16(e) shows the plot at M = 1.2 with maximum torque value of 20 Nm which occurred at the initial time of 0.013 sec.

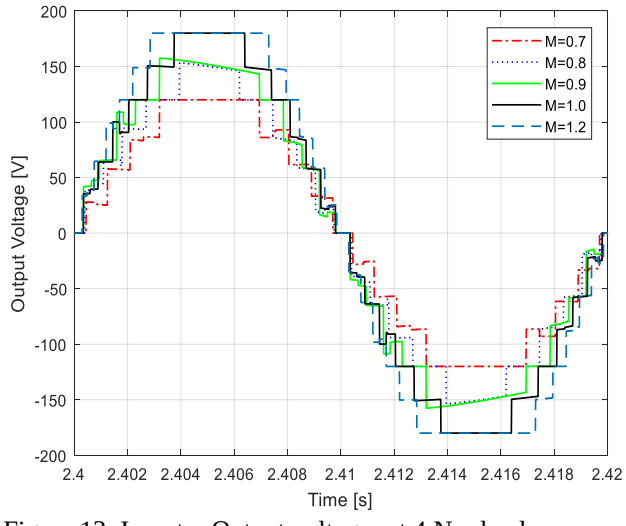

Figure 13: Inverter Output voltages at 4 Nm load

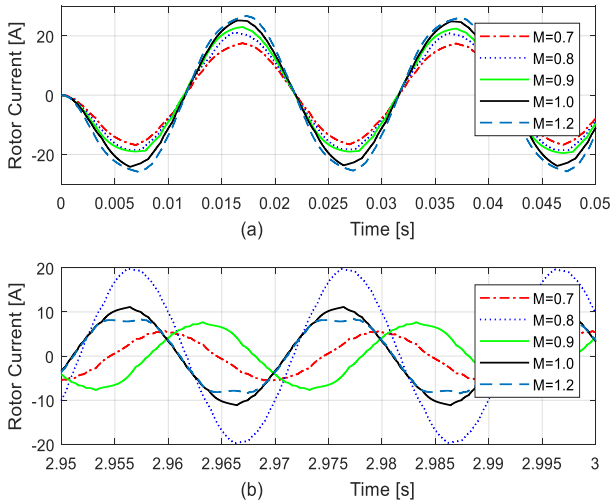

Figure 14: Inverter output current at 4 Nm load torque (a) transient (b) steady state.

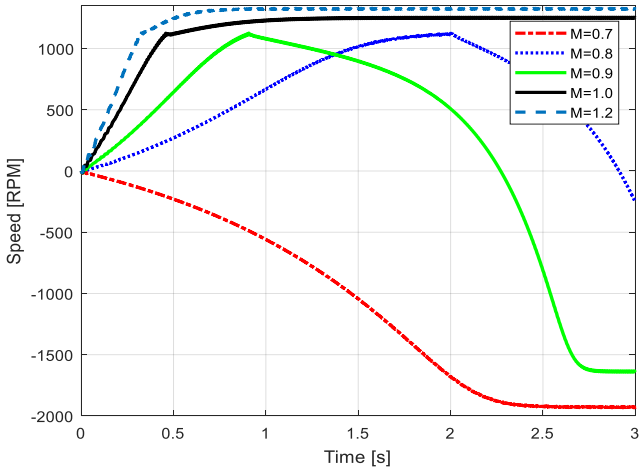

Figure 15: Motor speed at 4 Nm torque load

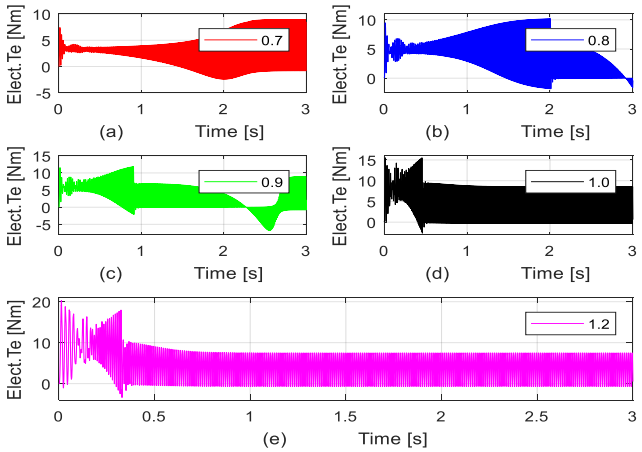

Figure 16: Electromagnetic torque under 4 Nm load condition.

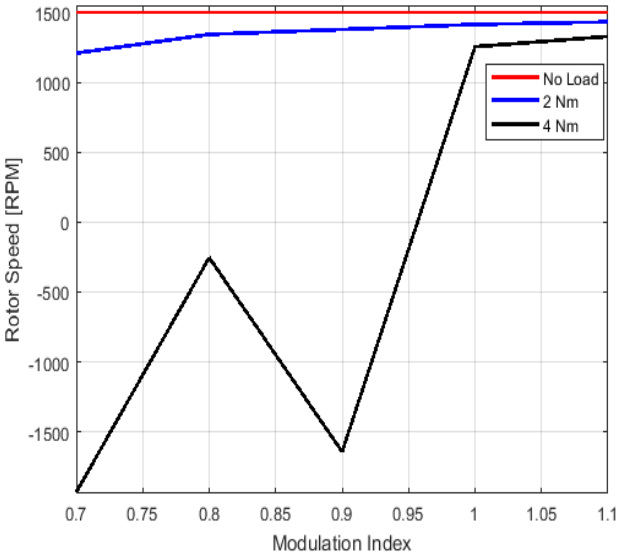

Figure 17: Motor rotor speed versus Modulation index waveform.

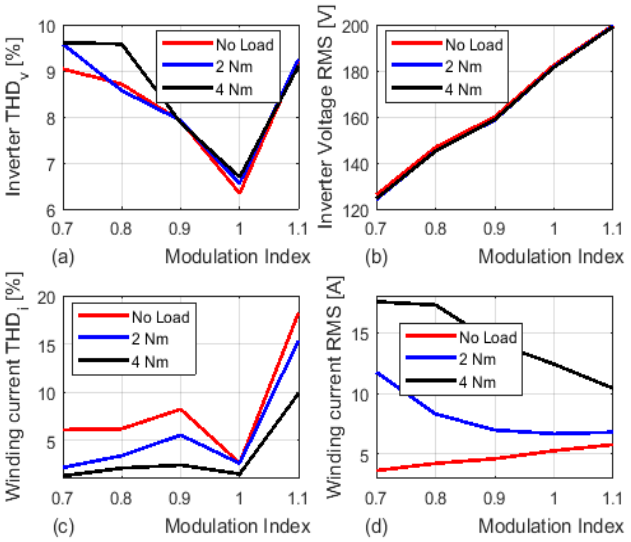

Figure 18: System Performance evaluation based on modulation index variation: (a) Inverter THDv (b) Voltage RMS (c) Winding THDi (d) Current RMS

Figure 17 displays the waveform rotor speed versus modulation index of the system. It is observed that at no load torque that the machine speed is not affected by the modulation index. At 2 Nm load torque, the rotor speed increases with increase in the modulation index. When the load torque increased to 4 Nm, the induction motor started from negative speed at modulation index value of 0.7 and moved to positive at M = 0.95 and remained positive up till M = 1.1. Figure 18 shows the system performance evaluation based on modulation index variation. Figure 18(a) depicts the waveforms of inverter voltage THD against modulation index, it is observed that all the different load values show THD that lies between 6.2 % – 6.7 % at M = 1.0. The inverter voltage RMS displays similar wave pattern at different load torque values as shown in Figure 18(b). Figure 18(c) depicts the waveforms of the machine winding current THD against modulation index at different load torques. Here, the 4 Nm load torque shows a better performance with less value of THD followed by 2 Nm and no load torque. The current RMS versus modulation index waveforms is displayed in Figure 18(d). It is observed that the winding current RMS value increases with increase in load torque values. The calculated and simulated switching angles are displayed in Table 3, this shows the angles at M = 1.2 and 0.8. They showed very close values of the switching angles.

Table 2: System parameters for MATLAB simulation

Parameter	**Value**
DC voltage for cell 1	60 V
DC voltage for cell 2	120 V
Fundamental Frequency	50 Hz
Nominal Power	0.25 ×746 VA

Parameter	Value
Voltage	240 V
Main Stator winding (R_s, L_{ls})	2.02 ohm, 7.4e^{-3} H
Main winding Rotor (R_r', L_{lr}')	4.12 ohm, 5.6e^{-3}H
Main winding mutual inductance (L_{ms})	0.1772 H
Auxiliary Winding stator (R_s, L_{ls})	7.14 ohm, 8.5e^{-3} H
Inertia, Pole pairs, turn (aux/main), (J, P, N_S/N_s)	0.0146 Kg.m^2, 2, 1.18
Capacitor-Start (R_{st}, C_s)	2 ohm, 254.7e^{-6} Farad

Table 3: Calculated and simulated switching angles

Switching angles	Modulation Index, M=1.2		Modulation Index, M= 0.8	
	Calculated (Roshini et al., 2021) (^{o})	Simulated (^{o})	Calculated (Roshini et al., 2021) (^{o})	Simulated (^{o})
θ_1	4.78	5.40	5.74	7.20
θ_2	14.48	13.50	17.46	19.80
θ_3	24.62	21.60	30.00	32.40
θ_4	35.69	30.60	44.43	48.60
θ_5	48.58	39.60	64.16	71.10
θ_6	66.44	51.30		

4. CONCLUSION

This work provides a study of effect of modulation index on cascaded multilevel inverter fed single phase induction motor using nearest level control technique. The simulated and calculated firing angles showed much similarity as depicted in Table 3. It is vividly clear from the result analysis that as the modulation index is varied from the range 0.7 to 1.2, under different load torque of zero, 2 Nm and 4 Nm. It is observed that the motor speed settling time varies proportional to the modulation index value increase. The system performed optimally at load torque of 2 Nm under modulation index of 1.0 resulting to 6.7 % and 4.5 % voltage and current THD respectively. The increase on load torque with low modulation index value affects the performance of the induction motor as improper selection of values can put the induction motor into generating mode. This study has revealed the loading limit of the selected motor and also provides the best modulation value that will deliver better harmonic content to the motor. These specific results will prolong the life span of the machine when properly selected.

REFERENCES

[1] Singh, V., Pattnaik, S., Gupta, S. & Santosh, B., (2016), A Single-Phase Cell-Based Asymmetrical Cascaded Multilevel inverter, *Journal of Power electronics*, 16(2), 532 – 541.

[2] Rodriguez, J., Franquelo, L. G., Kouro, S. J., Leon, I., Portillo, R. C., M. Prats, M. A. M. & Perez, M. A.,(2009), Multilevel converters: An enabling technology for high-power applications, *Proc. IEEE*, 97(11), 1786–1817.

[3] Kouro S., Malinowski, M., Gopakumar, K., Pou, J., Franquelo, L. G., Wu, B., Rodriguez, J., Perez, M. A., & Leon, J. I., (2010), Recent advances and industrial applications of multilevel converters, *IEEE Trans. Ind. Electron.*, 57(8), 2553–2580.

[4] Mohd Ain, N. A., Saleh, W. A. & Halim, W. A., (2020), Voltage harmonics reduction in single phase 9-level transistor clamped H-bridge inverter using nearest level control method, *Indonesian Journal of Electrical Engineering and Computer Science*, 20(3), 1725-1732.

[5] Cao, J. & Emadi, A., (2012), A new battery/ultra-capacitor hybrid energy storage system for electric, hybrid, and plug-in hybrid electric vehicles, *IEEE Transaction on Power Electronics*, 27(1), 122–132.

[6] Nithya, C. & Sangeetha, K., (2017), Single Phase Multilevel Inverter for Induction Motor Drives, International *Journal of Innovative Research in Electrical, Electronics, Instrumentation and Control Engineering*, 5(1), 104 – 113.

[7] Baptista, Bruno R. O., Mendes, Antre M. S., & Cruz, Sergio M. A., (2015), Thermal analysis and efficiency of an induction motor driven by a fault-tolerant multilevel Inverter Using FEM, *international Journal for Computation and Mathematics in Electrical and Electronic Engineering*, 34(2), 573 – 589.

[8] Subramanyam, M. V., Kuchibhatla, S. Mani & Prased, P. V. N., (2013), Effect of carrier Frequency on THD in Closed Lood Control of 5- level Multilevel Inverter fed 3-Phase induction Motor Drive, *International Journal of Scientific & Engineering Research*, 4(5), 804 – 809.

[9] Bahram, R. (2010), Speed Control Simulation for induction Motor by Multilevel VSI-fed to analyze current harmonics and Selective Harmonic Elimination, *Journal of Applied Sciences*, 10(8), 688-698.

[10] Muetze, A. & Binder, A., (2007), Calculation of circulating bearing currents in machines of inverter-based drive systems, *IEEE Trans. Ind. Electron.*, 54(2), 932–938.

[11] Matthew V. & Balaji G. (2012), A Novel Multilevel Inverter Topology for Induction Motor Drive, *International Journal of Innovative Research & Development*, 1(8), 504 – 519.
[12] Sivakumar, K., Das, A., Ramchand, R., Patel, C. & Gopakumar, C. (2009), A simple five-level inverter topology for induction motor drive using conventional two-level inverters and flying capacitor technique, *in 2009 35th Annual Conference of IEEE Industrial Electronics*, 1009–1013.
[13] Mahesh P., Venkatesh C. & Rajagopal V. (2021), NLC and SFO Control Technique Based Multilevel Inverter fed 3-φ induction Motor Drive, *International Conference on Sustainable Energy and Future Electric Transportation (SeFeT), 2021*, 253 – 270.
[14] Bonnett, A. H. (1996), Analysis of the Impact of Pulse-Width Modulated Inverter Voltage Waveforms on AC Induction Motors, *IEEE Trans. Ind. Appl*., 32(2), 386–392.
[15] Singh, V., Pattnaik, S., Gupta, S. & Santosh, B., (2016), A Single-Phase Cell-Based Asymmetrical Cascaded Multilevel inverter, *Journal of Power electronics*, 16(2), 532 – 541.
[16] McGrath, B. P., Holmes, D. G., Manjrekar, M. D. & Lipo, T. A., (2000), An improved modulation strategy for a hybrid multilevel inverter, in *Conference Record of the 2000 IEEE Industry Applications Conference, 2000,* 4, 2086-2093, 8-12.
[17] McGrath, B. P., & Holmes, D. G., (2002), Multicarrier PWM strategies for multilevel inverter" , in *IEEE Transactions on Industrial Electronics*, 49(4), 858-867.
[18] Wang, Y., Li, H., Shi, X., & Xu, B. (2004), A novel carrier-based PWM strategy for hybrid multilevel inverters, in *IEEE 35th Annual Power Electronics Specialists Conference*, 2004. PESC ’04. 6, 4233-4237, 20-25.
[19] Ayob, S, M., Yee, C. H., Muhamad, N. D. & Jusoh, A., (2005), A new hybrid multilevel inverter topology with harmonics profile improvement, in *International Conference on Power Electronics and Drives Systems, 2005. EDS 2005*, 2, 999 – 1002.
[20] Zhang, J., Zou, Y., Zhang, X., & Ding, K. (2001), Study on a modified multilevel cascade inverter with hybrid modulation, *Proceedings IEEE International Conference on Power Electronics and Drive Systems*, 2001, 1, 379-383.
[21] Rech, C., & Pinheiro, R. J. (2005), Impact of hybrid multilevel modulation strategy on input and output harmonic performances, Twentieth Annual IEEE Applied Power Electronics Conference and Exposition, 2005. APEC 2005, 1, 444-450.
[22] Liserre, M., Pigazo, A., Monopoli, V. G., Dell’Aquila, A. & Moreno, V. M., (2005), A generalized hybrid multilevel modulation technique developed in case of non-integer ratio among the dc-Link voltages, *Proceedings of the IEEE International Symposium on Industrial Electronics*, 2005. ISIE 2005, 2, 513 – 518.
[23] Perez, K. M., Rodriguez, J., Pontt, J. & Kouro, S., (2007), Power Distribution in Hybrid Multi-cell Converter with Nearest Level Modulation, *IEEE Int. Symp. Ind. Electron*, 736–741.
[24] Saleh, W. A., Said, N. A. & Halim, W. A., (2020), Harmonic Minimization of a Single-Phase Asymmetrical TCHB Multilevel Inverter based on Nearest Level Control Method, *International Journal of Power Electronics and Drive System*, 11(3), 1406 – 1414.
[25] Satputaley, R. J., Borghate, V. B., Kumar, V., & Kumar, T., (2017), Experimental Investigation of New Three-Phase Five Level Transistor Clamped H-bridge Inverter, *EPE Journal*, 27(1), 31 – 42.
[26] Roshini C. & Sreekumar C. (2021), Analysis of Symmetrical multilevel Inverter Driving Induction Motor, *International Conference on System Energy and Environment*, 2021, 299 – 303.
[27] Gopal K. D. (2009), Fundamentals of Electrical Drives, Narosa Publishing House, New Delhi Chennai Mumbai Kolkata, 23 - 30.